Selective Harmonic Elimination in Reduced-Switch Multilevel Inverters for PV Systems Using the Sparrow Search Algorithm

Saif Mohamed Baraa [1], Hazry Desa [2], Karar Saeed Mohammed [3], Taha Abdulsalam Al-Malaisi [4*], Abadal-Salam Taha Hussain [5], Hasan S. Majdi [6]
[1] Technical College of Engineering, Al-Bayan University, Baghdad, Iraq
[2, 4] Centre of Excellence for Unmanned Aerial Systems (COEUAS), Universiti Malaysia Perlis, Jalan Kangar-Alor Setar, 01000 Kangar, Perlis, Malaysia
[3] Department of Medical Physics, Almanara College for Medical Sciences, Iraq
[4] Renewable Energies Researches Unit, Northern Technical University, Iraq
[5] Department of Medical Instrumentation Techniques Engineering, Technical Engineering College, Al-Kitab University, Altun Kupri, Kirkuk, Iraq
[6] Department of Chemical Engineering and Petroleum Industries, Al-Mustaqbal University College, 51001 Hillah, Babylon, Iraq
Email: [1] dr.saifalsabti@gmail.com, [2] hazry@unimap.edu.my, [3] karar.s.mohammed@uomanara.edu.ia, [4] almalaisipi@gmail.com, [5] asth2233@gmail.com, [6] dr.hasanshker@mustaqbal-college.edu.iq
*Corresponding Author

***Abstract*—International Medium voltage and high-power systems use MLIs with low harmonic distortion voltage wave forms in medium voltage systems. Nevertheless, implementation of conventional MLI topologies appears to face various issues such as enhanced system complexity, costs, and conduction losses for specific switching frequencies as well as increased switching frequency leading to impractical solutions in RE systems. Based on the above analysis, this work introduces a three-phase, seven-level RS MLI topology applicable to photovoltaic (PV) systems. The proposed RS MLI has fewer switch devices than a typical topology to achieve cost optimizations without compromising the features of precise topologies. In an attempt to improve on the design of the RS MLI, the Selective Harmonic Elimination (SHE) method is implemented to minimize THD and switching losses. Iterative solutions can be delicate depending on the configuration of the SHE's and more so for higher level configurations. Thus, for solving the problem the Sparrow Search Algorithm (SSA), is developed to serve as the new optimization method. SSA is thus compared with Genetic Algorithm (GA) and Particle Swarm Optimization (PSO) using MATLAB/SIMULINK simulations with modulation indices of 0.1, 0.5 and 1.0. It is established from the result that proposed strategic swarm approach (SSA) yields better accuracy, fast convergence speed and improves the THD of the system compared to GA and PSO. However, there is still the question of computational complexity, which seems to entail studying the RS MLI in different conditions as an open problem for future work. The innovation made by this work can help to enhance RS MLI designs to better feasible for use in renewable energy systems.**

Keywords*—*Selective Harmonic Elimination (SHE); Reduced-Switch Multilevel Inverter; Photovoltaic (PV) Systems; Sparrow Search Algorithm (SSA); Harmonic Optimization.

I. INTRODUCTION

Most countries nowadays focus on the development of renewable energy sources which in turn has created the need for sophisticated and efficient power conversion systems that can easily incorporate renewable energy sources into present day power systems. When comparing renewable technologies, PV technologies appear to be one of the most promising mainly because of the great potential, scalability, and environmental performance. However, the operation of PV system largely depends on the evolution of efficient power electronics converters required for improving the energy conversion efficiency, reliability and quality of the delivered power [1]–[3].

Multilevel inverters have proved to be a critical inversion technology for medium voltage and high-power applications because of their suitability to produce improved output voltage wave forms with reduced harmonics distortion and low voltage stress across the power switching devices [4], [5]. There is significant performance improvement with the conventional MLI topologies such as diode clamped, capacitor clamped and cascaded H-bridge. But these systems exist with certain drawbacks which include the very many components, high costs, larger physical sizes and high switch losses. These disadvantages make them less suitable for use in renewable energy systems since the later requires simplicity, low cost, and high efficiency. To counter these difficulties, multilevel inverters of the reduced switch type (RS MLIs) have been introduced; these have comparatively slighter designs, are cheaper, and have fewer losses than traditional MLI [6]–[10].

While RS MLIs appear to have theoretical benefits, there are practical problems that are still largely unrecognized and scientifically unstudied in the context of actual PV systems. Issues like performance of the MLIs under varying load conditions, whether environmental factors have significant effects on the performance of the inverter and reliability concerns for long term application must be effectively addressed to unlock the full potential of RS MLIs. Also, total harmonic distortion (THD) in the output voltage waveform is still a crucial parameter of RS MLIs because high THD adversely affects the efficiency and reliability of equipment and grid operations [11]. Selective Harmonic Elimination (SHE) is one of the most common techniques implemented for harmonic suppression, because it allows the suppression of some lower order harmonic, maintaining at the same time the fundamental voltage amplitude [12]. However, solving the nonlinear equations of SHE is an optimization problem especially for higher level inverter connection.

In this respect, optimization algorithms have served as the backbone of solving SHE equations. Conventional techniques like the GA [13] and PSO [14] have been extensively adopted, but issue with slow convergence to global optimum, accuracy of solution, and lack of efficiency in terms of computer operations when facing problems with large number of parameters. Other metaheuristic techniques which have been developed are Simulated Annealing (SA) [15], Red Deer Algorithm (RDA) [16], Differential Evolution (DE) [17], and Artificial Bee Colony (ABC) [18]. Yet, these techniques lack some features such as entrapment into a local optimum, long time convergence or computational complexity.

The Sparrow Search Algorithm (SSA), an emerging optimization technique that mimics the feeding behavior of sparrows has been found to offer promising solutions to this challenge. SSA's forceful GSD, fast convergence and its capacity to solve nonlinear and high order problems make it fitting and well-suited for configuration problem such as SHE [19]-[26].

In this work, the concern is on the design, simulation, and improvement of a three-phase, seven-level RS MLI interfacing with a PV system [27]-[32]. The proposed RS MLI configuration is a cost-effective solution with least number of switching components in highly improved study as compared to basic topologies [33]-[36]. In order to boost the performance, the new SSA based SHE is used for the technique decreasing THD and switching loss as well as providing reliable operation. To compare the performance and superiority of the proposed SSA-based approach with GA- and PSO-based methods, a comparative study is performed [37]-[40].

MATLAB/SIMULINK is used to model and simulate the proposed system, and evaluation of the performance is done based on the remarks made above and for modulation index of 0.1, 0.3, 0.5, 0.7, 0.9 and 1. From the results it can be confirmed that significant enhancement in harmonic reduction, switching efficiency and overall performance of the system is achieved with the proposed SSA based SHE technique. Of value to the field of RS MLI designs and optimization, this work provides a foundation for further development of methodologies that enhance the integration of RE resources into power systems [41]-[47].

II. Approach to the Problem and Methodology

The Reduced Switch Multilevel Inverter (RS-MLI) maintains the performance advantages of traditional multilevel inverters (MLIs) while offering a more efficient and cost-effective solution by using fewer switching components. While traditional MLIs use multiple switching elements and passive components to achieve higher voltage levels, the RS-MLI operates with fewer components to achieve the same output voltage [48]-[53]. This makes the inverter more compact and cost-effective, while also simplifying the system and enhancing its efficiency. By reducing the voltage load on the switches, the seven-level reduced switch multilevel inverter circuit improves safety against overvoltage and dV/dt breakdown problems [54]-[58].

Fig. 1 depicts the setup of the RS MLI system, while Fig. 2 exhibits the output voltage waveform of the proposed RS MLI with its associated switching states. The RS MLI configuration seen in Fig. 2 utilizes seven switches (S11-S14 and S1-S3) together with two diodes (D1 and D2) [59]-[67].

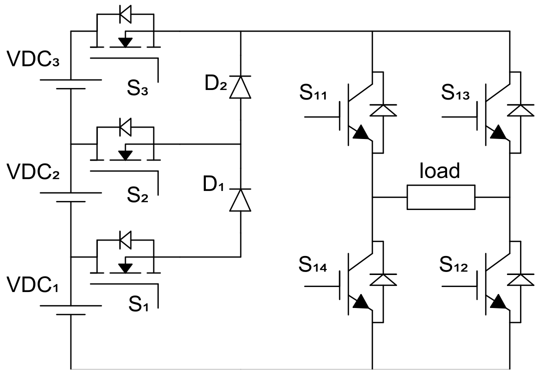

Fig. 1. Single phase seven-level reduced switch multilevel inverter [20]

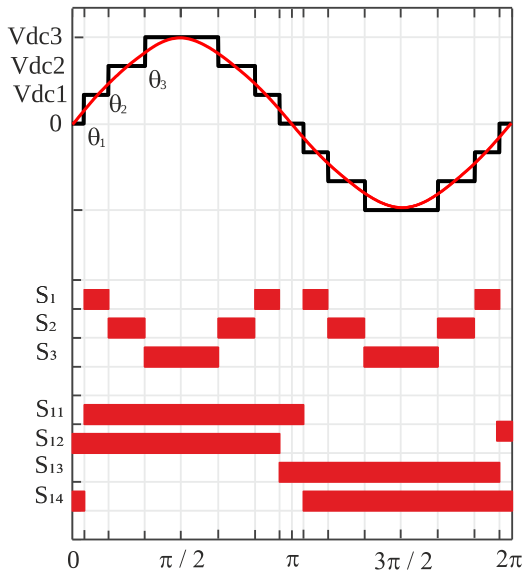

Fig. 2. Output voltage waveform and associated switching states of a single-phase seven-level RS-MLI [20]

In this setup, the H-bridge switches, which generate polarity, run at a low switching frequency, while the level generation switches (S1-S3) operate at a high switching frequency. To attain a cost-efficient design, low-frequency power components are used for the H-bridge, while high-frequency power components are employed for level generation. The operating concept of the RS MLI is delineated in the following scenarios. The operation of the suggested RS MLI for producing various output voltage levels is shown in Fig. 2, and the related switching mechanism is presented in Table I [20]:

- **Case a:** Switch S1, is ON (1), flow of current is through diode D1, and D2, and switches S11 and S12.The output voltage across the load is +VDC1.
- **Case b:** S13 and S14 are switched ON, output voltage across load is –VDC1.
- **Case c:** When switch S2 is turned ON, current flows through diode D2 and switches S11 and S12. As a result, the output voltage across the load is + (VDC1 + VDC2).
- **Case d:** S13 and Sl4 are switched ON, output voltage across load is – (VDC1 + VDC2).
- **Case e:** When switch S3 is ON, current flows through switches S11 and S12, while diodes D1 and D2 are reverse biased. As a result, the output voltage across the load is +(VDC1 + VDC2++ VDC3).
- **Case f:** S13 and S14 are switched ON, voltage output is – (VDC1 + VDC2+VDC3).
- **Case g:** S11 and S13 are activated, resulting in S1, S2, and S3 being deactivated (0), which yields a zero-voltage output across the load.
- **Case h:** S12 and S14 are activated, resulting in S1, S2, and S3 being deactivated (0), which yields a zero-voltage output across the load.

III. Mathematical Model of SHE-PWM for RS MLI

Selective Harmonic Elimination (SHE) is a low-frequency PWM approach. The SHE modulation technique controls the fundamental voltage while eliminating selected low-order harmonics from the corresponding voltage signal. After applying the SHE-PWM technique, a small and straightforward filter can eliminate the remaining high-order harmonics. In the SHE-PWM technique, the required nonlinear harmonic equations can be constructed using the Fourier expansion of the output voltage. Equation (2) can include all harmonic components in the expression of the output voltage. where, VDC1, VDC2, and VDC3 are the input voltages. $\theta 1$, $\theta 2$, and $\theta 3$ are the switching angles and due to quarter-wave symmetry, the switching angles must satisfy the constraint given by Eq. (1).

$$0 \le \theta_1 < \theta_2 < \theta_3 \le \frac{\pi}{2} \tag{1}$$

The first equation in Eq. (3) controls the magnitude of the fundamental voltage. The remaining equations are used to eliminate the selected harmonics. In balanced three-phase systems, the third harmonic and its multiples are naturally eliminated. Therefore, in this study, the values of V_5 and V_7 will be considered.

$$\begin{aligned} V_{fund} &= V_{\mathrm{DC1}}\, cos(\theta_1) + V_{\mathrm{DC3}}\, cos(\theta_2) \\ &\quad + V_{\mathrm{DC3}}\, cos(\theta_3) \\ V_5 &= V_{\mathrm{DC1}}\, cos(5\theta_1) + V_{\mathrm{DC3}}\, cos(5\theta_2) \\ &\quad + V_{\mathrm{DC3}}\, cos(5\theta_3) \\ V_7 &= V_{\mathrm{DC1}}\, cos(7\theta_1) + V_{\mathrm{DC3}}\, cos(7\theta_2) \\ &\quad + V_{\mathrm{DC3}}\, cos(7\theta_3) \end{aligned} \tag{3}$$

Solving nonlinear equations can be extremely challenging. However, using evolutionary algorithms, which define a specific objective function, can overcome this challenge. In the 7-level three-phase RS-MLI (Fig. 3), the fitness function is defined in Eq. (4) to adjust the magnitude of the fundamental component to the desired value and eliminate the selected harmonics.

$$f = \min_{\theta_i}\{|V_{1p} - V_{\mathrm{ref}}| + |V_5| + |V_7|\} \tag{4}$$

Here, V_{1p} represents the output voltage obtained when the calculated angles are applied to the driver. V_{ref} is the desired reference voltage, and %ε denotes the acceptable error tolerance, which is selected as 1% in this study.

In the SHE technique, control of the fundamental voltage is achieved through the modulation index. Eq. (5) defines the modulation index (M) as the proportion of the desired peak value of the fundamental voltage to the total DC input voltage.

$$M = \frac{V_{1p}}{\sum V_{DC_i}} \tag{5}$$

$$V_{\mathrm{ab}}(\omega t) = \sum_{n=1,3,5,7,\ldots}^{\infty} \frac{4}{n.\pi} * [V_{DC_1}\, cos(n\theta_1) + \mathrm{V}_{DC_2}\, cos(n\theta_2) + \mathrm{V}_{DC_3}\, cos(n\theta_3)] * [sin(nwt)] \tag{2}$$

TABLE I. Switching Schemes of 7-level RS MLI

Switching state	S_1	S_2	S_3	S_{11}	S_{12}	S_{13}	S_{14}	D_1	D_2
V_{DC3}	0	0	1	1	0	0	0	×	×
V_{DC2}	0	1	0	1	1	0	0	×	✓
V_{DC1}	1	0	0	1	1	0	0	✓	✓
0	0	0	0	1	0	1	0	×	×
0	0	0	0	0	1	0	1	×	×
$-V_{DC1}$	1	0	0	0	0	1	1	✓	✓
$-V_{DC2}$	0	1	0	1	0	0	1	×	✓
$-V_{DC3}$	0	0	1	0	0	1	1	×	×

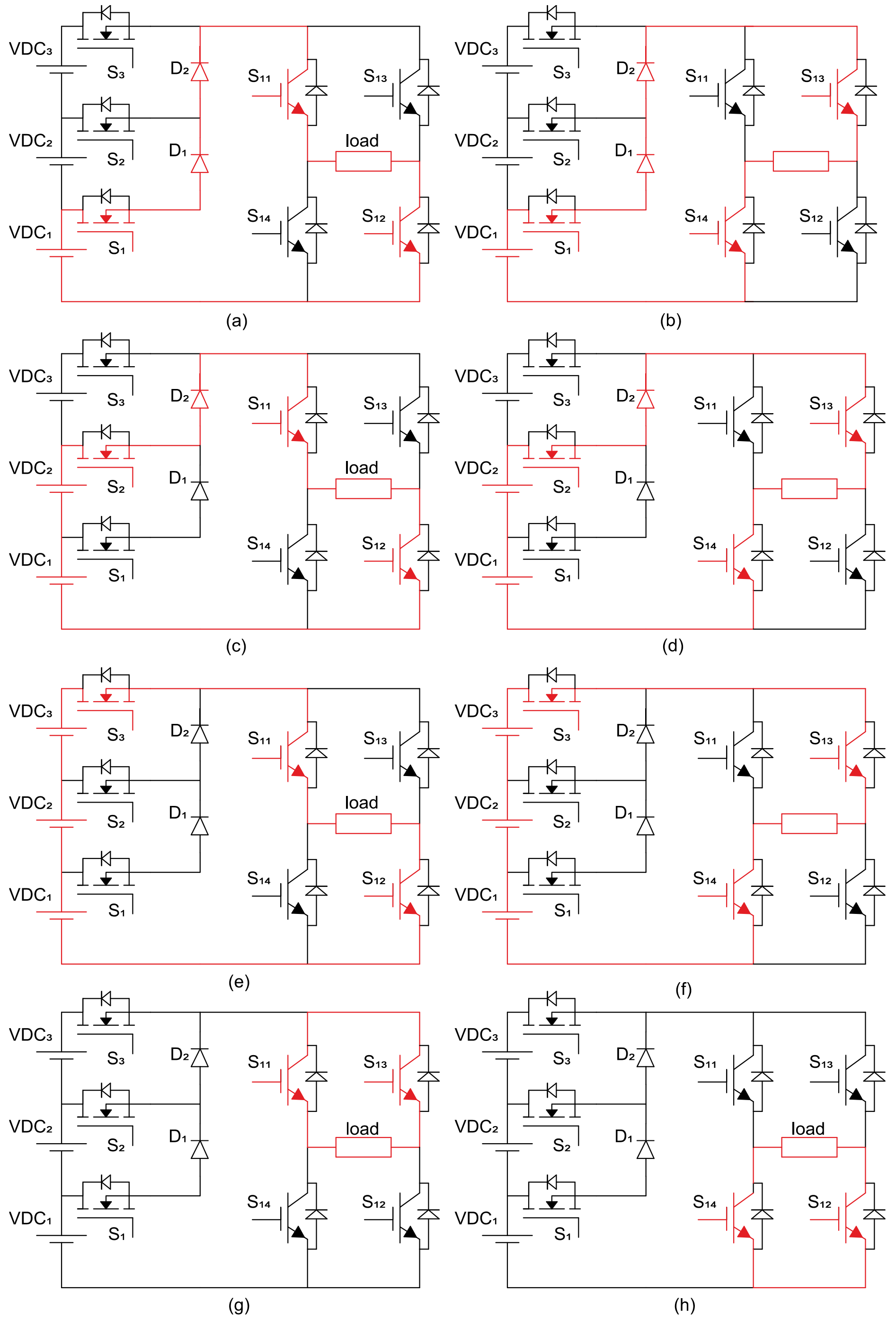

Fig. 3. RS MLI setup for producing various output voltage levels: (a) case a: + Vdc1, (b) case b: – Vdc1; (c) case c: + (Vdc1+ Vdc2), (d) case d: – (Vdc1+ Vdc2), (e) case e: + (Vdc1+ Vdc2+ Vdc3), (f) case f: – (Vdc1+ Vdc2+ Vdc3), (g) case g: 0, (h) case h: 0

Total Harmonic Distortion (THD) is a measure of the total harmonic content in a signal relative to its fundamental frequency component. It quantifies the degree to which a waveform deviates from a pure sinusoidal shape due to the presence of harmonics. In power systems, a low THD indicates high power quality, while a high THD can reduce system efficiency and potentially harm connected equipment. Mathematically, THD is defined as:

$$THD = \sqrt{\frac{\sum_{n=2}^{\infty} V_n^2}{V_1^2}} \tag{5}$$

$$THD = \frac{\sqrt{V_5^2 + V_7^2 + \ldots + V_{49}^2}}{|V_1|} \tag{7}$$

$$THD = \frac{\sqrt{V_5^2 + V_7^2}}{|V_1|} \tag{8}$$

Where, V_n, RMS value of the n-th harmonic component, V_1, RMS value of the fundamental frequency component. THD is typically expressed as a percentage and is a key parameter for evaluating the purity and quality of electrical waveforms in various applications. In three-phase systems, harmonics that are multiples of 3 are typically ignored. Additionally, the calculation of Total Harmonic Distortion (THD) usually considers harmonics up to the 49th order.

Therefore, Equation (6) can be revised and expressed as Equation (7). For THDe, only the 5th and 7th harmonics are considered [68]-[73].

IV. Photovoltaic Integrated Three-Phase Reduced Switch Multilevel Inverter

Fig. 4 illustrates the arrangement of the PV-based three-phase seven-level RS MLI system that is explored in this study. Incremental Conductance (IC) Maximum Power Point Tracking (MPPT) approach, a DC-DC boost converter, and the RS MLI design are used in order to incorporate photovoltaic panels. When conventional multilayer inverters (MLIs) are used, the Total Harmonic Distortion (THD) that they produce is often larger. As a consequence, the use of large filters is required in order to mitigate this phenomenon [21]. Furthermore, the number of components required for traditional MLIs increases as the voltage levels rise, prompting researchers to explore alternative topological designs for improved performance [74]-[80].

V. Proposed SSA-based SHE-PWM Method

A. Sparrow Search Algorithm (SSA)

Sparrow Search Algorithm (SSA) is one of the recent developments in nature inspired swarm-based algorithm and proposed by Xue and Shen [19]. SSA is based on how sparrows, the subject of social simulation, behave when they are searching for food and how these birds work in teams. Many works have reported investigating SSA performance, comparing it to other optimization methods. Regarding the rates of convergence, the mathematical expectations of the convergence speeds have stable and encouraging results that SSA frequently surpasses in many optimization problems other algorithms of the mentioned group. For instance, SSA has been implemented to deal with the engineering problems like the power systems optimization, the parameters' estimation in the control systems, and manufacturing process enhancement. However, research and practical experience with SSA show that, in addition to high performance, it offers relatively easy configurability and has fewer control parameters compared with other metaheuristic algorithms, thus making it available to researchers and professionals of various fields. In the SSA algorithm, sparrows have learned behaviors that are crucial in their day-to-day existence. These behaviors include:

- The algorithm divides sparrows into two categories: producers and searchers. The producers are also involved in the searching for foods or in looking for raw food or figures of a potential food direction, as illustrated in Fig. 5. Instead, searchers are interested in finding sources of food that have been located by producers themselves.
- Sparrows show a defensive posturing as they move about in search of food. For this reason, a sub SPEA of sparrows is chosen to be called "scouters" that hunt for the predators to alert the rest. Observers use alarms when they see danger, such that producers and searchers can move away from the risky zone.

The population has therefore an effective switching of roles among the producers and searchers aimed to maximize the discovery of the food sources. Yet, the number of producers and searchers combined does not change during this process either

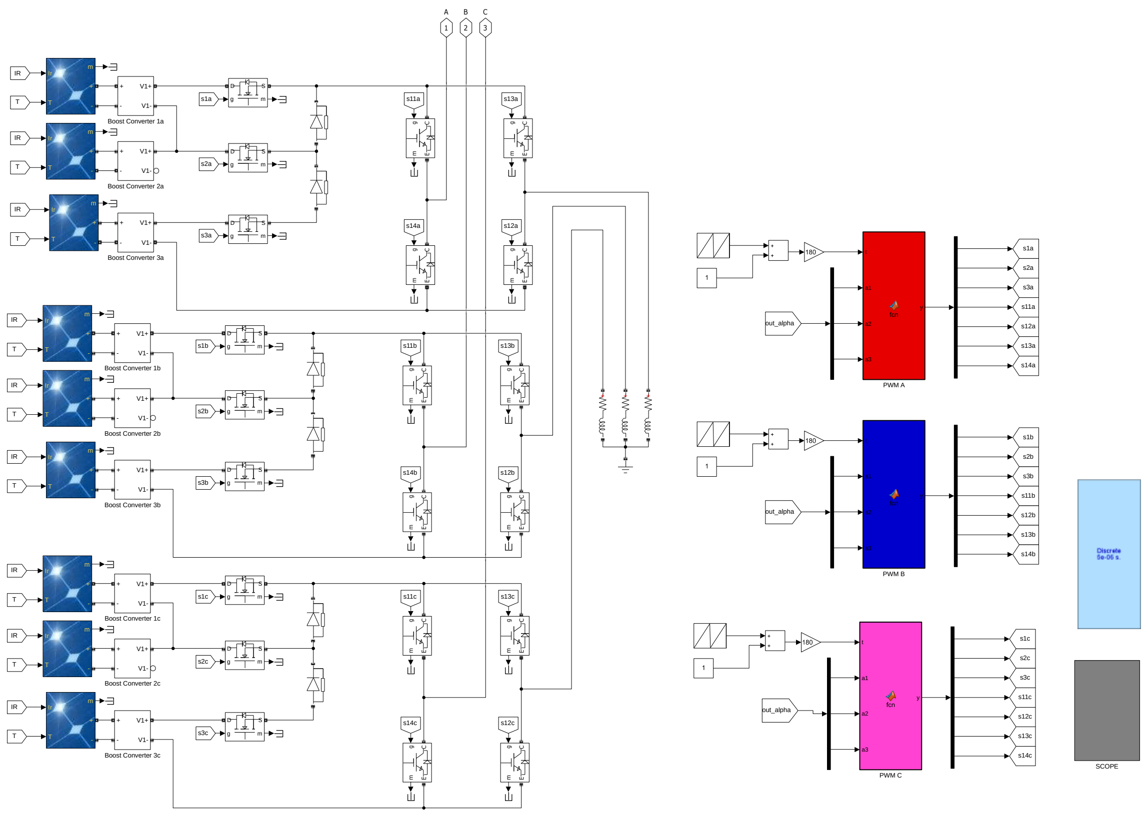

Fig. 4. Model of a Three-Phase Seven-Level RS-MLI Integrated with Photovoltaic Panels and a DC–DC Boost Converter constructed in MATLAB/Simulink

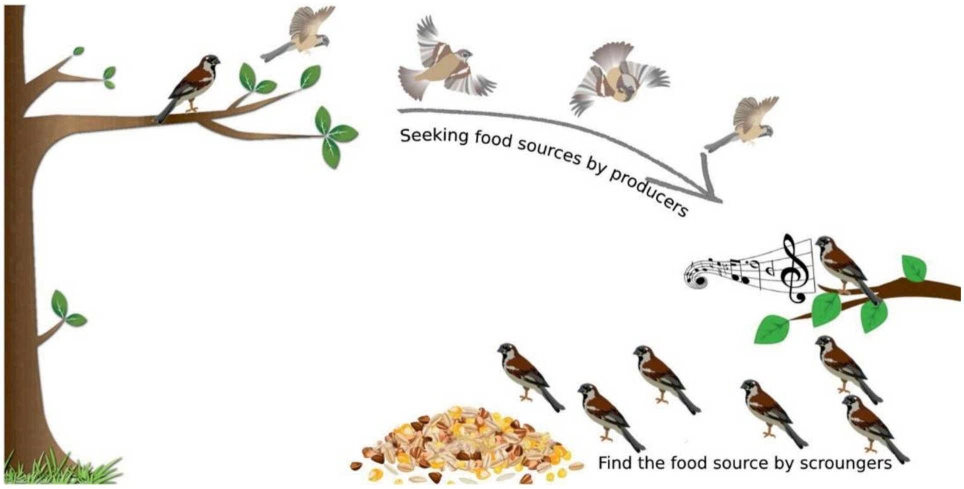

Fig. 5. Searching and finding food sources by growers and foragers [19]

Step 1: Prepare Steps for the SSA Algorithm Let the initial values of the Sparrow Search Algorithm (SSA) be initialized as; N and G_{max} are used to denote the population size and the maximum number of iterations respectively, while Np was the producer's population size, Ns was the searcher population size and Nsc was the scout population size respectively. Optimal choice of these parameters improves the flow of the algorithm as well as its effectiveness.

Step 2: Generate Initial Population in this step, the population is created the population is composed of N sparrows. The positions of the sparrows are described by matrices of size of $N \times D$, where D is the dimensionality of the search space (8). Every record of the matrix indicates the location of a sparrow, which is given by x_i = (x_i; 1, x_i; 2, ..., x_i; D). Here, ε and ξ means the j-th decision variable of the i-th sparrow, where j = 1, 2, …, D. The elements x_i, j are given random values within the bounds lbj (lower bound and ubj upper bound. The fitness of each position of sparrows is modeled using a fitness function with the representation $f(x_i$, j) for all $I \in (1, 2, \dots, N)$. Subsequently, the fitness values are computed and the position of the best sparrow in the population is decided and known as x^{Gbest}.

$$\text{Population} = \begin{bmatrix} x_{1,1} & x_{12} & x_{13} & \cdots & x_{1,D} \\ x_{2,1} & x_{22} & x_{23} & \cdots & x_{2,D} \\ \vdots & \vdots & \vdots & \ddots & \vdots \\ x_{N,1} & x_{N,2} & x_{N,3} & \cdots & x_{N,D} \end{bmatrix} \tag{8}$$

Step 3: Dividing the Total Population into Makers and Seekers the population is divided into two categories: producers and searchers. Producers are the most competent sparrows in the population in terms of food searching and directing other sparrows on where to find foods. The later, however, try to look for food based on the indications given by the producers. This distinction is not fixed, in that assignment to each group is changed during each iteration of the process. The variables g chosen as current and G_{max} as maximum iterations in line 2 and α is a random number between 0 and 1. $r \in [0, 1]$ is readjusted according to the values of $ST \in [0.5, 1]$, representing alarm and safety thresholds, while the random number Q of normal distribution is used. The vector L is initialized with all its elements to 1 and it will have the size of D. In the case of $r < ST$, the producers go on searching on their own. But if $r \geq ST$ all the sparrows are made to shift to safer regions because danger is inherent according.

Step 4: Update Sparrow Positions Sparrows' positions are adjusted through iterations in order to enhance their fitness. Producers update their positions in the market more so than the searchers do. The position update of the producers is calculated with the help of Equation (9) and searchers using Equation (10). Equation (10) is to show the change in the position of the least fit sparrow, and x^{Pbest} symbolizes the best position identified by the i-th producer. The vector A consists of D elements of which each of them has random numbers generated between 1 and -1. It is position adjustment matrix $A^{+} = AT\ (AAT)^{-1}$ that is used in the process. If $i > N/2$, the searcher must go to another area in the search for food and conversely if $i \geq N/2$ the searcher will try to look for food around the location of the best performing sparrows x^{Pbest}.

$$x_{i,j}(g+1) = \begin{cases} x_{i,j}(g) \times exp\left(\dfrac{-i}{\alpha \times G_{max}}\right) r < ST, \\ x_{i,j}(g) + Q \times Lr \geq ST. \end{cases} \tag{9}$$

$$x_{i,j}(g+1) = \begin{cases} Q \times exp\left(\dfrac{x_j^{\text{wors}} - x_{i,j}(g)}{i^2}\right) & i > \dfrac{N}{2}, \\ x_j^{\text{Pbest}} - \left|x_{i,j}(g) - x_j^{\text{Pbest}}\right| \times A^{+} \times L & i \leq \dfrac{N}{2}. \end{cases} \tag{10}$$

Step 5: Choose and Change Scout Officers as scouts who look for dangers, 10 to 20 percent of the populace is selected. The update of positions of these scouts is done applying Equation (11). In Equations (11) and (13) where x^{Pbest} is the best position found in the population and xworst is the worst. The value of $\delta\ \beta$ depends on the step size which is normally distributed within zero and one variance; and k is an arbitrary chosen figure which ranges from -1 to 1. Sparrows of the i-th order which have a value of $f(x_i(g)) > f(x^{Gbest})$ are considered to be unsafe position. On the other hand, when $f(x_i(g)) = f(x^{Gbest})$, it means the best candidate is toward the center of the swarm.

$$x_{i,j}(g+1) = \begin{cases} \psi^1, & f(x_i(g)) > f\left(x^{\text{Gbest}}\right), \\ \psi^2, & f(x_i(g)) = f\left(x^{\text{Gbest}}\right). \end{cases} \quad (11)$$

$$\psi^1 = x_j^{\text{Gbest}} + \beta \times \left| x_{i,j}(g) - x_j^{\text{Gbest}} \right| \quad (12)$$

$$\psi^2 = x_{i,j}(g) + K \times \left(\frac{x_{i,j}(g) - x_j^{\text{wors}}}{f(x_i(g)) - f(x^{\text{wors}}) + \rho} \right) \quad (13)$$

Step 6: Evaluate and Update Positions in every iteration, their position is changed if the new position enhances its fitness goal at that iteration. The old position is substituted by a new position $x_i(g+1)$ if $f(x_i(g+1)) < f(x_i(g))$ for all sparrows in the population, $i \in (1, 2, \dots, N$.

Step 7: Update Best Sparrow Position after updating the sparrow positions, the next step is to check a fitness of the new position is less than the fitness of the global best solution $f(x_i(g+1))$ Then, update the global best position x^{Gbest}.

Step 8: Check Termination Condition perform steps 3 to 7 set until the number of iterations times G has arrived maximum allowed of iterations G_{max}. If G_{max} iterations have been completed the algorithm stops.

VI. Test and Results

The optimization of the SHE equations for the three-phase 7-level RS-MLI configuration was tested in the MATLAB Simulink environment using GA, PSO, and BO algorithms. For each algorithm, simulations were independently conducted ten times, with 50 individuals and 100 iterations per run. The best solutions obtained were then used to simulate the results over the modulation index range from 0 to 1 in MATLAB Simulink. The SSA optimization code provided in [19] was modified to apply to the multilevel harmonic elimination problem and was implemented using MATLAB software. The simulations were performed on a laptop with an AMD Ryzen 9 7845HX processor (5.2 GHz), 32.0 GB RAM, and a GeForce RTX™ 4070 NVIDIA graphics card. The simulation results are presented in Table II for GA, Table III for PSO, and Table IV for SSA.

TABLE II. Switching Angles Calculated with GA

GA-SHE										
m	**θ_1**	**θ_2**	**θ_3**	**Vref(max)**	**V1p(rms)**	**error (%)**	**THD (%)**	**THD (%)**	**5th (%)**	**7th (%)**
0.10	84.282	86.116	86.116	15.00	14.97	0.20%	220.06	135.91	97.46	94.74
0.20	64.114	87.949	90.000	30.00	29.98	0.07%	53.45	40.96	40.38	6.86
0.30	47.441	89.152	89.152	45.00	44.86	0.31%	30.51	17.65	11.08	13.73
0.40	46.811	75.688	89.381	60.00	59.87	0.22%	19.96	9.40	8.84	3.20
0.50	41.310	65.088	89.668	75.00	74.82	0.24%	17.31	2.44	0.69	2.34
0.60	42.170	58.900	81.016	90.00	89.77	0.26%	13.67	3.96	3.69	1.46
0.70	16.329	49.332	87.834	105.00	104.70	0.29%	15.46	2.68	0.72	2.54
0.80	0.057	28.476	89.668	120.00	119.70	0.25%	13.88	2.52	2.52	0.13
0.90	14.152	38.847	68.182	135.00	134.60	0.30%	12.11	4.87	2.87	3.94
1.00	8.652	30.309	59.759	150.00	149.6	0.27%	9.06	2.97	2.79	1.04

TABLE III. Switching Angles Calculated with PSO

PSO-SHE										
m	**θ_1**	**θ_2**	**θ_3**	**Vref(max)**	**V1p(rms)**	**Error (%)**	**THD (%)**	**THD (%)**	**5th (%)**	**7th (%)**
0.10	76.433	89.970	89.970	15.00	14.97	0.20%	109.58	99.94	79.13	61.04
0.20	62.038	90.000	90.000	30.00	29.80	0.67%	38.45	28.77	27.55	8.28
0.30	52.739	87.094	87.094	45.00	44.95	0.11%	46.07	12.52	11.04	5.91
0.40	44.613	76.667	90.000	60.00	59.91	0.15%	16.94	6.35	3.99	4.95
0.50	40.741	65.669	89.517	75.00	74.39	0.81%	17.39	0.55	0.34	0.43
0.60	38.703	59.245	82.996	90.00	89.77	0.26%	11.31	1.71	0.61	1.60
0.70	38.432	54.034	73.818	105.00	104.70	0.29%	12.24	0.21	0.17	0.12
0.80	29.215	53.999	64.890	120.00	119.80	0.17%	10.53	0.30	0.23	0.20
0.90	17.464	43.060	64.149	135.00	134.70	0.22%	11.81	0.03	0.01	0.01
1.00	11.644	30.674	58.362	150.00	149.6	0.27%	7.71	0.68	0.60	0.32

TABLE IV. Switching Angles Calculated with SSA

SSA-SHE										
m	**θ_1**	**θ_2**	**θ_3**	**Vref(max)**	**V1p(rms)**	**Error (%)**	**THD (%)**	**THD (%)**	**5th (%)**	**7th (%)**
0.10	76.372	90.000	90.000	15.00	15.01	-0.07%	**109.13**	**99.51**	**79.08**	**60.41**
0.20	61.885	90.000	90.000	30.00	29.94	0.20%	**37.79**	**28.40**	**27.01**	**8.80**
0.30	51.218	85.383	90.000	45.00	44.90	0.22%	**32.97**	**10.38**	**4.36**	**9.42**
0.40	45.873	75.745	90.000	60.00	59.89	0.18%	**17.66**	**7.04**	**6.33**	**3.10**
0.50	40.769	65.826	89.356	75.00	74.87	0.17%	**17.46**	**0.09**	**0.04**	**0.08**
0.60	39.436	58.585	83.099	90.00	89.83	0.19%	**12.36**	**0.05**	**0.02**	**0.04**
0.70	38.337	53.937	73.962	105.00	104.80	0.19%	**12.25**	**0.03**	**0.01**	**0.03**
0.80	29.229	54.339	64.579	120.00	119.70	0.25%	**10.69**	**0.07**	**0.03**	**0.06**
0.90	17.507	43.052	64.141	135.00	134.60	0.30%	**11.82**	**0.02**	**0.01**	**0.01**
1.00	11.644	30.921	58.425	150.00	149.9	0.07%	**7.78**	**0.01**	**0.01**	**0.01**

The convergence curves of the three algorithms are shown in Fig. 6. The convergence curves reveal that SSA achieved the optimal value in only 27 iterations, showcasing the fastest convergence among the three algorithms. PSO reached its best solution at the 70th iteration, while GA achieved its optimal value at the 57th iteration. Although GA required fewer iterations than PSO, it produced the least effective result overall. In contrast, SSA not only converged more rapidly but also delivered the most accurate and efficient solution, demonstrating superior performance compared to the other algorithms. The switching angles obtained using GA, PSO, and SSA algorithms for low, medium, and high modulation indices were applied to the Simulink model of a three-phase seven-level RS-MLI in Fig. 4. The voltage waveforms generated for a modulation index of 1.0 using the GA, PSO, and SSA algorithms are presented in Fig. 7.

Fig. 8 presents the harmonic spectrum analyses of the GA, PSO, and SSA algorithms for a unit modulation index. When the switching angles determined by the GA were applied to the inverter, the fundamental voltage value was obtained as 149.6 V (max) with a 0.27% error, and the THD value of the load voltage was measured at 9.06% (Fig. 8(a)). The PSO algorithm achieved a fundamental voltage of 150.1 V (max) with a 0.07% error and a THD value of 7.85% (Fig. 8(b)). Finally, the SSA algorithm yielded a fundamental voltage of 149.9 V (rms) with 0.07% error and a THD value of 7.78% (Fig. 8(c)). Fig. 9 illustrates the harmonic suppression performance of various algorithms for specific harmonics. As shown in Fig. 9(a), the THD value achieved using the GA algorithm is 2.97%. In Fig. 9(b), the THD is reduced to 0.12% with the application of the PSO algorithm. Lastly, in Fig. 6(c), the THD is calculated as 0.01% with the use of the SSA algorithm.

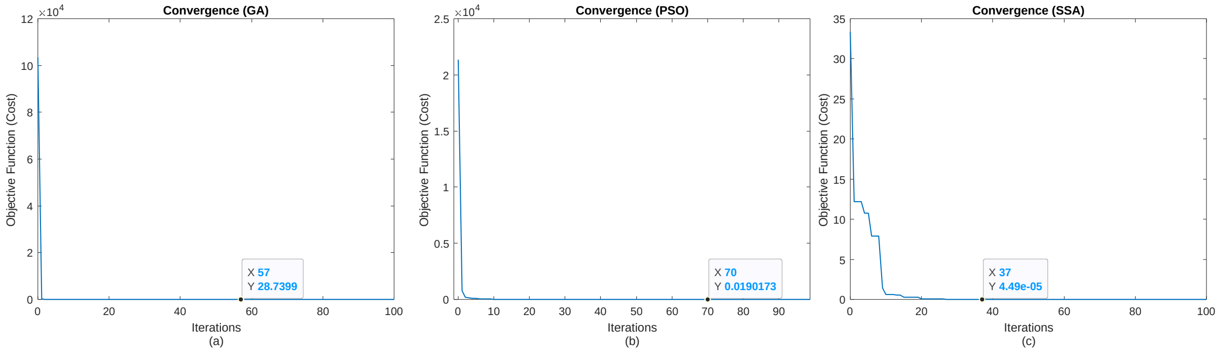

Fig. 6. Convergence Curves for a) GA, b) PSO, and c) SSA

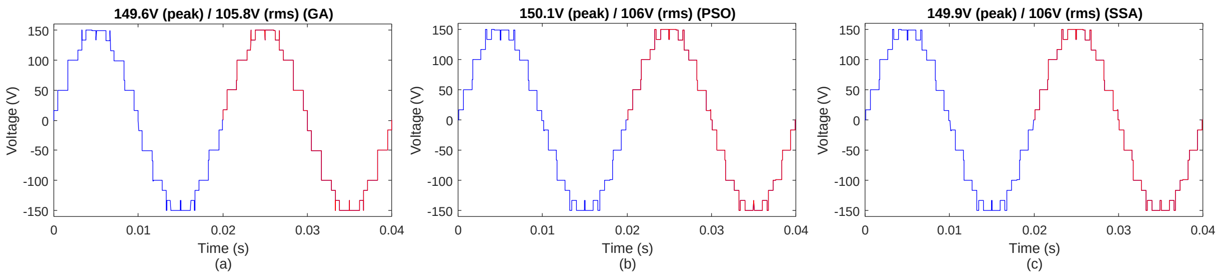

Fig. 7. Output Waveforms of the Inverter at Modulation Index M=0.1: a) GA, b) PSO, c) SSA

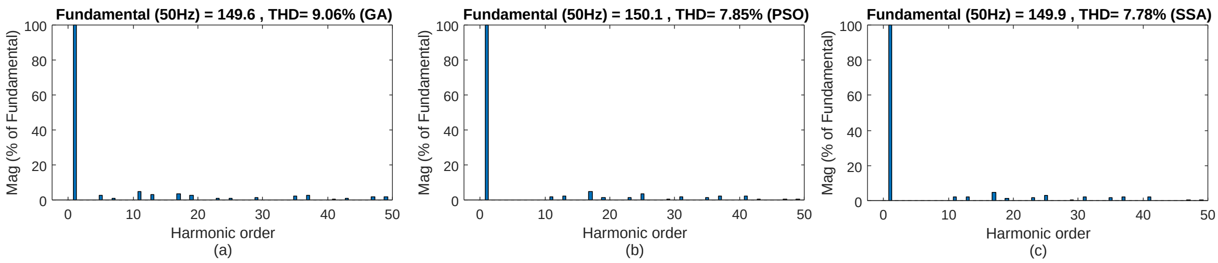

Fig. 8. THD analysis for M=0.1 a) GA, b) PSO, and c) SSA

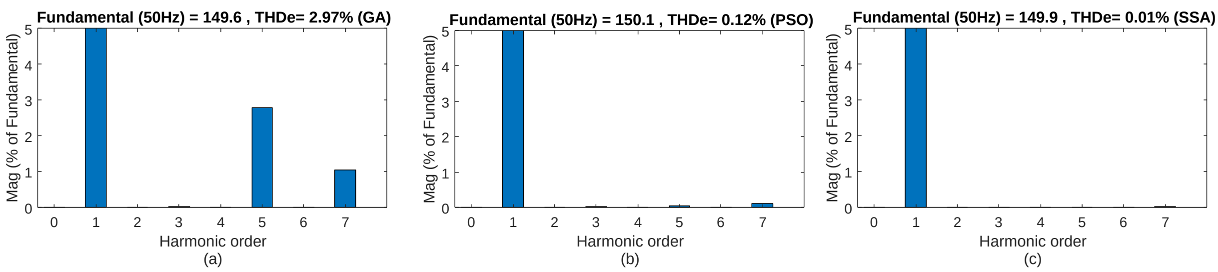

Fig. 9. THDe analysis for M=0.1 a) GA, b) PSO, and c) SSA

VII. Conclusion

This research offers an extensive analysis of three optimization algorithms namely Genetic Algorithm (GA), Particle Swarm Optimization (PSO), and Salp Swarm Algorithm (SSA) in an application of a three phase, seven level Reduced Switch Multilevel Inverter (RS-MLI) for Selective Harmonic Elimination (SHE). The following outcomes revealed that SSA converges much faster, works with greater accuracy while suppress the harmonic more efficiently comparing with GA and PSO. In particular, the optimal solution has been determined in 27 iterations by SSA, which is less than GA with 57 iterations and PSO with 70 iterations while providing the best solutions with least harmonics distortion. These reporting suggests the possibility of using SSA in improving inverter efficiency, especially for high-power and renewable energy systems.

However, few limitations can be considered while inferring from these results. First, the study mainly considered the performance of SSA under definite experimental input such as exact population sizes and numbers of iterations. We did not investigate on how SSA response to these parameters such as population size, iteration count, and modulation index range. Highly specific information on ratios of convection and radiation heat transfer coefficients and other parameters could be explored in the future to examine the effects of these parameters on the efficiency of SSA and define how SSA may best be configured to operate under various conditions. Moreover, all the results presented in this work were obtained under controlled circumstances and additional experiments are needed to assess SSA's performance for real-world scenarios with fluctuating loads, temperature and system noise.

However, SSA was shown to deliver better harmonic attenuation than the PI loop, and the experiment did not consider the possibility of overfitting the signals, nor was it carried out with different types of inverters or when applied to various applications. The above findings show that there is a research potential to analyze the performance of SSA under different environ and combining SSA with other optimization methods to improve its reliability and performance. Further, the extent to which SSA can be employed for other formats of MLI and for more extensive and diverse applications in high power, complicated structures should be investigated.

The SSA can be used synergistically to other control strategies in order to enhance its feasibility in practice especially with respect to situations where fine-tuned, dynamic and responsive control systems are required. In the future work, it might be interesting to examine the interaction of SSA with other optimization algorithms as DE or ABC, in order to improve the performance of the method in various optimization problems.

This research enriches the existing literature in the field of optimization techniques for the design of multilevel inverters, making an argument that SSA enables improved harmonic mitigation and the quicker convergence of results. In applying SSA for SHE problems, the engineers and researchers can enhance the performance of the multilevel inverters appropriate for high quality renewable energy systems and power electronics applications. It is suggested that SSA holds a unique potential for targeting optimization issues in multilevel inverter applications, is therefore indicated that future work will investigate the real-life applicability and synergistic use of SSA with other optimizations techniques. Future work should cover the aforementioned limitations, and we encourage the researchers to study SSA's performance in more complex scenarios including dynamic loads and real-time control to assess its effectiveness in real world inverter designs.

Acknowledgment

Publication fund incentive from Universiti Malaysia Perlis (UniMAP). Saif Mohamed Baraa expresses his appreciation to Al-Bayan University which has offered the equipment and the opportunities that enable this study by Al-Bayan University, Technical College of Engineering, Baghdad – 10011, Iraq.

References

[1] Q. Zhang *et al*., "Control and Intelligent Optimization of a Photovoltaic (PV) Inverter System: A Review," *Energies*, vol. 17, no. 7, p. 1571, 2024.

[2] U. Mustafa, I. A. Qeays, M. S. BinArif, S. M. Yahya, and S. B. Md. Ayob, "Efficiency improvement of the solar PV-system using nanofluid and developed inverter topology," *Energy Sources, Part A: Recovery, Utilization, and Environmental Effects*, vol. 46, no. 1, pp. 14657-14673, 2024.

[3] Z. Q. S. Nwokediegwu, K. I. Ibekwe, V. I. Ilojianya, E. A. Etukudoh, and O. B. Ayorinde, "Renewable energy technologies in engineering: A review of current developments and future prospects," *Engineering Science & Technology Journal*, vol. 5, no. 2, pp. 367-384, 2024.

[4] S. Munawar, M. S. Iqbal, M. Adnan, M. Ali Akbar, and A. Bermak, "Multilevel Inverters Design, Topologies, and Applications: Research Issues, Current, and Future Directions," in *IEEE Access*, vol. 12, pp. 149320-149350, 2024.

[5] A. A. Khan, A. F. Minai, Q. Alam, and F. I. Bakhsh, "Multilevel Inverters: Classification, Approaches, and Its Application in Photovoltaic System," *Multilevel Converters*, pp. 27-50, 2024.

[6] A. Sirsa, A. Mittal, and A. Ojha, "A novel reconfigurable reduced switch multilevel inverter for renewable applications," *Electrical Engineering*, pp. 1-15, 2024.

[7] P. J. Choi, J. Lee, and A. Jang, "Interconnection between renewable energy technologies and water treatment processes," *Water Research*, p. 122037, 2024.

[8] P. R. Bana, K. P. Panda, R. T. Naayagi, P. Siano, and G. Panda, "Recently developed reduced switch multilevel inverter for renewable energy integration and drives application: topologies, comprehensive analysis and comparative evaluation," *IEEE access*, vol. 7, pp. 54888-54909, 2019.

[9] V. K. NV, "A comprehensive survey on reduced switch count multilevel inverter topologies and modulation techniques," *Journal of Electrical Systems and Information Technology*, vol. 10, no. 1, p. 3, 2023.

[10] Y. Bektaş, "Real-time control of Selective Harmonic Elimination in a Reduced Switch Multilevel Inverter with unequal DC sources," *Ain Shams Engineering Journal*, vol. 15, no. 6, p. 102719, 2024.

[11] M. P. Selvam, S. K. Palraj, and G. S. Madasamy, "Adaptive control of a single source reduced switch MLI-based DSTATCOM for wind energy conversion system," *Electrical Engineering*, pp. 1-22, 2024.

[12] M. S. Dahidah, G. Konstantinou, and V. G. Agelidis, "A review of multilevel selective harmonic elimination PWM: formulations, solving algorithms, implementation and applications," *IEEE Transactions on Power Electronics*, vol. 30, no. 8, pp. 4091-4106, 2014.

[13] H. Karaca and E. Bektaş, "GA based selective harmonic elimination for multilevel inverter with reduced number of switches," *methods*, vol. 9, p. 10, 2015.

[14] M. Sadoughi, A. Pourdadashnia, M. Farhadi-Kangarlu, and S. Galvani, "PSO-optimized SHE-PWM technique in a cascaded H-bridge

multilevel inverter for variable output voltage applications," *IEEE Transactions on Power Electronics*, vol. 37, no. 7, pp. 8065-8075, 2022.

[15] V. K. Chinnaiyan, M. Pradish, and S. P. Karthikeyan, "Simulated annealing based selective harmonic elimination for multi-level inverter," *Energy Procedia*, vol. 117, pp. 855-861, 2017.

[16] Y. Bektaş and H. Karaca, "Red deer algorithm based harmonic mitigation for asymmetric cascaded multilevel inverters," in *2022 57th International Scientific Conference on Information, Communication and Energy Systems and Technologies (ICEST)*, pp. 1-4, 2022.

[17] Z. Salam and N. Bahari, "Selective harmonics elimination PWM (SHEPWM) using differential evolution approach," in *2010 Joint International Conference on Power Electronics, Drives and Energy Systems & 2010 Power India*, pp. 1-5, 2010.

[18] M. H. Arshad, B. Ismail, M. Z. Aihsan, W. A. Mustafa, H. A. Rahim, and R. H. C. Alfith, "Performance Analysis of Modified Nine-level Inverter with SHEPWM using an Artificial Bee Colony Algorithm," *2021 4th International Iraqi Conference on Engineering Technology and Their Applications (IICETA)*, pp. 162-167, 2021.

[19] J. Xue and B. Shen, "A novel swarm intelligence optimization approach: sparrow search algorithm," *Systems science & control engineering*, vol. 8, no. 1, pp. 22-34, 2020.

[20] Y. Gopal, D. Birla, and M. Lalwani, "Reduced switches multilevel inverter integration with boost converters in photovoltaic system," *SN Applied Sciences*, vol. 2, pp. 1-15, 2020.

[21] N. Prabaharan and K. Palanisamy, "Analysis and integration of multilevel inverter configuration with boost converters in a photovoltaic system," *Energy Convers Manag*, vol. 128, pp. 327–342, 2016.

[22] S. M. Khazaal and H. Maarouf, "Predicting Coronary Artery Disease Utilizing Support Vector Machines: Optimizing Predictive Model," *Mesopotamian Journal of Artificial Intelligence in Healthcare*, vol. 2023, pp. 21-26, 2023.

[23] A. M. Abdel-Hamed, A. M. Nasser, H. Shatla, and A. Refky, "An improved SPWM control approach with aid of ant lion optimization for minimizing the THD in multilevel inverters," *Scientific Reports*, vol. 15, no. 1, p. 1990, 2025.

[24] V. Govindan, J. Jayaprakash, C. Park, J. R. Lee, and I. N. Cangul, "Optimization-Based Design and Control of Dynamic Systems," *Babylonian Journal of Mathematics*, vol. 2023, pp. 30-35, 2023.

[25] A. Singh, V. Jately, P. Kala, and Y. Yang, "Enhancing power quality in electric vehicles and battery energy storage systems using multilevel inverter topologies–A review," *Journal of Energy Storage*, vol. 110, p. 115274, 2025.

[26] N. M. Sivaram, "Design and optimization of automotive cardan shafts for industrial applications with enhanced performance and durability," *Babylonian Journal of Mechanical Engineering*, vol. 2023, pp. 1-12, 2023.

[27] K. Balasubramani and U. M. Natarajan, "A fuzzy wavelet neural network (FWNN) and hybrid optimization machine learning technique for traffic flow prediction," *Babylonian Journal of Machine Learning*, vol. 2024, pp. 121-132, 2024.

[28] M. S. Hossain *et al*., "Performance Evaluation of a Nearest Level Control-Based TCHB Multilevel Inverter for PMSM Motors in Electric Vehicle Systems," *Results in Engineering*, p. 103949, 2025.

[29] M. Al-Mukhtar, A. A. Abbas, A. H. Hamad, and M. H. Al-hashimi, "Normalized-UNet Segmentation for COVID-19 Utilizing an Encoder-Decoder Connection Layer Block," *Journal of Image and Graphics*, vol. 12, no. 1, 2024.

[30] H. Mansourizadeh, M. Hosseinpour, A. Seifi, and M. Shahparasti, "A 13-level switched-capacitor-based multilevel inverter with reduced components and inrush current limitation," *Scientific Reports*, vol. 15, no. 1, p. 290, 2025.

[31] J. Chouhan, P. Gawhade, A. Ojha, and P. Swarnkar, "A comprehensive review of hybrid energy systems utilizing multilevel inverters with minimal switch count," *Electrical Engineering*, pp. 1-25, 2024.

[32] V. Govindaraj, S. Mayakrishnan, S. Venkatarajan, R. Raman, and R. Sundar, "Design and development of photovoltaic solar system based single phase seven level inverter," *Bulletin of Electrical Engineering and Informatics*, vol. 13, no. 1, pp. 58-66, 2024.

[33] I. Ahamad *et al*., "Performance assessment of solar energy driven cascaded H-bridge multilevel inverters," *Microsystem Technologies*, pp. 1-9, 2024.

[34] Y. Wang, J. Ye, R. Ku, Y. Shen, G. Li, and J. Liang, "A modular switched-capacitor multilevel inverter featuring voltage gain ability," *Journal of Power Electronics*, vol. 23, no. 1, pp. 11-22, 2023.

[35] A. H. Hamad, A. A. Mahmood, S. A. Abed, and X. Ying, "Semantic relatedness maximisation for word sense disambiguation using a hybrid firefly algorithm," *Journal of Intelligent & Fuzzy Systems*, vol. 41, no. 6, pp. 7047-7061, 2021.

[36] F. Esmaeili and H. R. Koofigar, "Single-Phase Switched-Capacitor 21-Level Inverter Topology Using Reduced Number of Components With High Voltage Gain," in *IEEE Access*, vol. 12, pp. 192979-192989, 2024.

[37] X. Ying and A. H. Hamad, "A hybrid bat algorithm based on combined semantic measures for word sense disambiguation," in *Advances in Natural Computation, Fuzzy Systems and Knowledge Discovery*, vol. 1, pp. 149-157, 2020.

[38] J. Kasinath *et al*., "A Novel Three-Phase Switched-Capacitor Five-Level Multilevel Inverter with Reduced Components and Self-Balancing Ability," *Applied sciences (Basel)*, vol. 13, no. 3, pp. 1-19, 2023.

[39] T. Hai *et al*., "DependData: Data collection dependability through three-layer decision-making in BSNs for healthcare monitoring," *Information Fusion*, vol. 62, pp. 32-46, 2020.

[40] G. M. Oorappan, S. Pandarinathan, and J. Arumugam, "A new nine-level switched-capacitor-based multilevel inverter with low voltage stress and self-balancing," *Electrical Engineering*, vol. 105, no. 2, pp. 867-882, 2023.

[41] S. K. Bhagat *et al*., "Evaluating physical and fiscal water leakage in water distribution system," *Water*, vol. 11, no. 10, p. 2091, 2019.

[42] Y. Hu, R. Naderi, and Y. Naderi, "A switched-capacitor based multilevel inverter with reduced circuit components and voltage boosting capability," *International Transactions on Electrical Energy Systems*, vol. 31, no. 8, p. e12990, 2021.

[43] S. Q. Salih, A. A. Alsewari, B. Al-Khateeb, and M. F. Zolkipli, "Novel multi-swarm approach for balancing exploration and exploitation in particle swarm optimization," in *Recent Trends in Data Science and Soft Computing: Proceedings of the 3rd International Conference of Reliable Information and Communication Technology (IRICT 2018)*, pp. 196-206, 2019.

[44] J. Liu, J. Wu, X. Zhu, and J. Zeng, "A switched-capacitor multilevel inverter with reduced power components in current loops for renewable energy generation," *Electric Power Components and Systems*, vol. 47, no. 9-10, pp. 876-888, 2019.

[45] S. A. M. Al-Juboori, F. Hazzaa, Z. S. Jabbar, S. Salih, and H. M. Gheni, "Man-in-the-middle and denial of service attacks detection using machine learning algorithms," *Bulletin of Electrical Engineering and Informatics*, vol. 12, no. 1, pp. 418-426, 2023.

[46] M. Hosseinpour, M. Derakhshandeh, A. Seifi, and M. Shahparasti, "A 17-level quadruple boost switched-capacitor inverter with reduced devices and limited charge current," *Scientific Reports*, vol. 14, no. 1, p. 6233, 2024.

[47] H. Guo, H. Tao, S. Q. Salih, and Z. M. Yaseen, "Optimized parameter estimation of a PEMFC model based on improved Grass Fibrous Root Optimization Algorithm," *Energy Reports*, vol. 6, pp. 1510-1519, 2020.

[48] Z. Xun, H. Ding, and Z. He, "A novel switched-capacitor inverter with reduced capacitance and balanced neutral-point voltage," *Electronics*, vol. 10, no. 8, p. 947, 2021.

[49] A. S. T. Hussain, F. H. Taha, H. A. Fadhil, S. Q. Salih, and T. A. Taha, "Designing an optimal PID controller for a PV-connected Zeta converter using genetic algorithm," *International Journal of Power Electronics and Drive System (IJPEDS)*, vol. 15, no. 2, pp. 566-576, 2024.

[50] V. Anand and V. Singh, "A 13-Level Switched-Capacitor Multilevel Inverter With Single DC Source," in *IEEE Journal of Emerging and Selected Topics in Power Electronics*, vol. 10, no. 2, pp. 1575-1586, April 2022.

[51] S. Q. Salih *et al*., "Enhanced Total Harmonic Distortion Optimization in Cascaded H-Bridge Multilevel Inverters Using the Dwarf Mongoose

Optimization Algorithm," *Journal of Robotics and Control (JRC)*, vol. 5, no. 6, pp. 1862-1871, 2024.

[52] M. A. Hosseinzadeh, M. Sarebanzadeh, C. F. Garcia, E. Babaei, J. Rodriguez, and R. Kennel, "Reduced Multisource Switched-Capacitor Multilevel Inverter Topologies," in *IEEE Transactions on Power Electronics*, vol. 37, no. 12, pp. 14647-14666, Dec. 2022.

[53] T. A. Taha, N. I. A. Wahab, M. K. Hassan, and H. I. Zaynal, "Selective Harmonic Elimination in Multilevel Inverters Using the Bonobo Optimization Algorithm," in *International Conference on Forthcoming Networks and Sustainability in the AIoT Era*, pp. 304-321, 2024.

[54] V. Anand *et al*., "Seventeen Level Switched Capacitor Inverters With the Capability of High Voltage Gain and Low Inrush Current," in *IEEE Journal of Emerging and Selected Topics in Industrial Electronics*, vol. 4, no. 4, pp. 1138-1150, Oct. 2023.

[55] E. Bektaş *et al*., "Enhancing Harmonic Reduction in Multilevel Inverters using the Weevil Damage Optimization Algorithm," *Journal of Robotics and Control (JRC)*, vol. 5, no. 3, pp. 717-722, 2024.

[56] Y. Wang, J. Ye, C. Zhou, Y. Shen, W. Liu, and J. Liang, "A switched-capacitor multilevel inverter using series-parallel conversion with reduced components," *CPSS Transactions on Power Electronics and Applications*, vol. 7, no. 3, pp. 335-346, 2022.

[57] Y. Bektaş, H. Karaca, T. A. Taha, and H. I. Zaynal, "Red deer algorithm-based selective harmonic elimination technique for multilevel inverters," *Bulletin of Electrical Engineering and Informatics*, vol. 12, no. 5, pp. 2643-2650, 2023.

[58] Z. Deng, X. Zhu, J. Duan, J. Ye, and Y. Wang, "A Multilevel Switched Capacitor Inverter with Reduced Components and Self-Balance," *Applied Sciences*, vol. 13, no. 15, p. 8955, 2023.

[59] O. K. Ahmed, S. Algburi, M. A. Jasim, T. A. Taha, A. M. Saleh, and K. F. Yassin, "Experimental assessment of the effect of black dye and water depth on the performance of PV/solar distiller," *Desalination and Water Treatment*, vol. 318, p. 100317, 2024.

[60] M. Amani, M. N. Azari, and M. Rezanejad, "Single source self-balanced switched-capacitor multilevel inverter with reduced number of semiconductors," *IET Power Electronics*, vol. 16, no. 4, pp. 575-583, 2023.

[61] H. Juma'a and T. Atyia, "Design and Implementation of multi-level inverter for PV system with various DC Sources," *NTU Journal of Renewable Energy*, vol. 5, no. 1, pp. 24-33, 2023.

[62] E. H. I. Albajari and S. R. Aslan, "Exploring the Synergy of Integration: Assessing the Performance of Hydraulic Storage and Solar Power Integration in Kirkuk city," *NTU Journal of Renewable Energy*, vol. 5, no. 1, pp. 1-7, 2023.

[63] A. K. Singh and R. K. Mandal, "A Novel 17-Level Reduced Component Single DC Switched-Capacitor-Based Inverter With Reduced Input Spike Current," in *IEEE Journal of Emerging and Selected Topics in Power Electronics*, vol. 10, no. 5, pp. 6045-6056, Oct. 2022.

[64] Z. Ali, Z. M. Abdullah, B. A. Naser, R. W. Daoud, and A. H. Ahmed, "Design of a Single-Phase Inverter for Solar Energy Conversion System," *NTU Journal of Renewable Energy*, vol. 1, no. 1, pp. 38-42, 2021.

[65] H. Aghaei, S. M. Hashemzadeh, E. Babaei, M. B. B. Sharifian, and A. Iqbal, "An extendable switched-capacitor based three-phase multilevel inverter with boosting capability," *IET Power Electronics*, vol. 17, no. 15, pp. 2601-2612, 2024.

[66] Z. N. Abdulhameed, H. I. Hamd, Y. K. Najm, and E. H. Yahia, "Evaluation of OFDM over a noisy channel based on transmitting multimedia data," in *AIP Conference Proceedings*, vol. 3009, no. 1, 2024.

[67] M. R. Hussan, A. Sarwar, I. Khan, M. Tariq, M. Tayyab, and W. Alhosaini, "An eleven-level switched-capacitor inverter with boosting capability," *Electronics*, vol. 10, no. 18, p. 2262, 2021.

[68] Y. Al Mashhadany, S. Jassam, and E. H. Yahia, "Design and Simulation of Modified Type-2 Fuzzy Logic Controller for Power System," *IJEER*, vol. 10, no. 3, pp. 731-736, 2022.

[69] K. Jena, K. K. Gupta, D. Kumar, N. K. Dewangan, and S. R. Kabat, "A 3-Φ switched-capacitor-based multilevel inverter with reduced voltage stress and part count," *Electrical Engineering*, vol. 106, no. 3, pp. 2679-2690, 2024.

[70] Y. Wang, J. Ye, R. Ku, Y. Wang, and J. Liang, "Novel extensible multilevel inverter based on switched-capacitor structure," *Journal of power electronics*, vol. 22, no. 9, pp. 1448-1460, 2022.

[71] A. F. Ataala *et al*., "A Hybrid GA-GWO Method for Cyber Attack Detection Using RF Model," *Journal of Cybersecurity & Information Management*, vol. 15, no. 1, 2025.

[72] P. Bhatnagar, R. Agrawal, and K. K. Gupta, "Reduced device count version of single-stage switched-capacitor module for cascaded multilevel inverters," *IET Power Electronics*, vol. 12, no. 5, pp. 1079-1086, 2019.

[73] W. Peng, Q. Ni, X. Qiu, and Y. Ye, "Seven-Level Inverter With Self-Balanced Switched-Capacitor and Its Cascaded Extension," in *IEEE Transactions on Power Electronics*, vol. 34, no. 12, pp. 11889-11896, Dec. 2019.

[74] M. Derakhshandeh, M. Hosseinpour, A. Seifi, and M. Shahparasti, "An enhanced 13-level triple voltage gain switched capacitor inverter with lower power electronics devices," *IET Power Electronics*, vol. 17, no. 14, pp. 1925-1942, 2024.

[75] M. H. Al-Jumaili, H. M. Haglan, M. K. Mohammed, and Q. H. Eesee, "An automatic multi-axis solar tracking system in Ramadi city: design and implementation," *Indonesian Journal of Electrical Engineering and Computer Science*, vol. 19, no. 3, pp. 1126-1234, 2020.

[76] H. K. Jahan, H. Tarzamni, P. Kolahian, S. H. Hosseini, F. Tahami, and F. Blaabjerg, "A Switched-Capacitor Inverter with Optimized Switch-count Considering Load Power Factor," *IECON 2019 - 45th Annual Conference of the IEEE Industrial Electronics Society*, pp. 4959-4964, 2019.

[77] K. Jena, C. K. Panigrahi, and K. K. Gupta, "A Single-Phase Step-Up 5-level Switched-Capacitor Inverter with Reduced Device Count," *2021 1st International Conference on Power Electronics and Energy (ICPEE)*, pp. 1-6, 2021.

[78] A. Taheri and H. Samsami, "New topology of a switched-capacitor-based multilevel inverter with a single DC power supply," *IET Power Electronics*, vol. 12, no. 6, pp. 1571-1584, 2019.

[79] P. R. Bana, K. P. Panda, S. Padmanaban, and G. Panda, "Extendable Switched-Capacitor Multilevel Inverter With Reduced Number of Components and Self-Balancing Capacitors," in *IEEE Transactions on Industry Applications*, vol. 57, no. 3, pp. 3154-3163, May-June 2021.

[80] B. Sharma, S. Manna, V. Saxena, P. K. Raghuvanshi, M. H. Alsharif, and M. K. Kim, "A comprehensive review of multi-level inverters, modulation, and control for grid-interfaced solar PV systems," *Scientific Reports*, vol. 15, no. 1, p. 661, 2025.